Scientific Report

SOURCE DATA | TRANSPARENT PROCESS

EMBO reports

SIRT5 promotes IDH2 desuccinylation and G6PD deglutarylation to enhance cellular antioxidant defense

Lisha Zhou[1,2,3,4,†], Fang Wang[1,2,3,4,†], Renqiang Sun[1,2,3,4], Xiufei Chen[1,2,3,4], Mengli Zhang[1,2,3,4], Qi Xu[1,2,3,4], Yi Wang[1,2,3,4], Shiwen Wang[1,2,3,4], Yue Xiong[1,2,3,4,5], Kun-Liang Guan[1,2,3,4,6], Pengyuan Yang[1,2,3,4], Hongxiu Yu[1,2,3,4,*] & Dan Ye[1,2,3,4,7,**]

Abstract

Excess in mitochondrial reactive oxygen species (ROS) is considered as a major cause of cellular oxidative stress. NADPH, the main intracellular reductant, has a key role in keeping glutathione in its reduced form GSH, which scavenges ROS and thus protects the cell from oxidative damage. Here, we report that SIRT5 desuccinylates and deglutarylates isocitrate dehydrogenase 2 (IDH2) and glucose-6-phosphate dehydrogenase (G6PD), respectively, and thus activates both NADPH-producing enzymes. Moreover, we show that knockdown or knockout of *SIRT5* leads to high levels of cellular ROS. SIRT5 inactivation leads to the inhibition of IDH2 and G6PD, thereby decreasing NADPH production, lowering GSH, impairing the ability to scavenge ROS, and increasing cellular susceptibility to oxidative stress. Our study uncovers a SIRT5-dependent mechanism that regulates cellular NADPH homeostasis and redox potential by promoting IDH2 desuccinylation and G6PD deglutarylation.

Keywords glutarylation; NADPH; oxidative stress; SIRT5; succinylation
Subject Categories Metabolism; Physiology; Post-translational Modifications, Proteolysis & Proteomics
DOI 10.15252/embr.201541643 | Received 24 October 2015 | Revised 29 February 2016 | Accepted 8 March 2016 | Published online 9 April 2016
EMBO Reports (2016) 17: 811–822

Introduction

Cellular damage caused by aberrant reactive oxygen species (ROS) is considered as a major cause in many age-related diseases. To prevent from ROS-induced damage, cells have developed a metabolic network to maintain intracellular levels of nicotinamide adenine dinucleotide phosphate (NADPH), a major cellular reductant, and thus a proper redox state. NADPH is commonly used to keep glutathione in its reduced form GSH, which scavenges ROS and converts harmful hydrogen peroxide to water with the help of glutathione peroxidase (GSHPx) [1]. In this process, GSH is oxidized to its disulfide, GSSG. Perturbed NADPH production disrupts cell division, increases cell sensitivity to ROS, and provokes apoptosis [2]. Major NADPH-producing enzymes are glucose-6-phosphate dehydrogenase (G6PD) and 6-phosphogluconate dehydrogenase (6PGD) in the pentose phosphate pathway (PPP), malic enzyme (ME) in the pyruvate cycling pathway, methylenetetrahydrofolate dehydrogenase 1 and 2 (MTHFD1/2) in the one-carbon metabolic pathway, and isocitrate dehydrogenase 1 and 2 (IDH1/2) which catalyzes the oxidative decarboxylation of isocitrate and produces alpha-ketoglutarate (α-KG) outside the context of the tricarboxylic acid cycle (TCA cycle). In addition to a critical role in maintaining NADPH homeostasis, IDH1 and IDH2 enzymes have recently received great attention because their mutated forms produce an oncometabolite 2-hydroxyglutarate, which can alter the epigenetic landscape by inhibiting multiple α-KG-dependent histone and DNA demethylases [3].

Large-scale proteomic surveys of cellular proteins have demonstrated that lysines can be posttranslationally modified by various types of acylations, including acetylation [4–6], succinylation [7], malonylation [8,9], glutarylation [10], crotonylation [11,12], propionylation [13], and butyrylation [13]. Among these posttranslational modifications, protein acetylation is the most well-studied regulatory mechanism for multiple metabolic processes [14,15]. To date, more than 4,500 acetylated proteins have been identified [16]. In addition, recent studies have discovered that succinylation, malonylation, and

1 Key Laboratory of Metabolism and Molecular Medicine, Ministry of Education, Fudan University, Shanghai, China
2 Department of Biochemistry and Molecular Biology, School of Basic Medical Sciences, Fudan University, Shanghai, China
3 State Key Laboratory of Genetic Engineering, Collaborative Innovation Center of Genetics and Development, School of Life Sciences, Fudan University, Shanghai, China
4 Molecular and Cell Biology Lab, Institute of Biomedical Sciences, Shanghai Medical College, Fudan University, Shanghai, China
5 Department of Biochemistry and Biophysics, Lineberger Comprehensive Cancer Center, University of North Carolina, Chapel Hill, NC, USA
6 Department of Pharmacology and Moores Cancer Center, University of California San Diego, La Jolla, CA, USA
7 Department of General Surgery, Huashan Hospital, Fudan University, Shanghai, China
*Corresponding author. Tel: +86 2154 237664; E-mail: hongxiuyu@fudan.edu.cn
**Corresponding author. Tel: +86 2154 237450; E-mail: yedan@fudan.edu.cn
†These authors contribute equally to this work

glutarylation, which are structurally similar, can also regulate metabolic pathways [10,17–20]. The potential presence of a transferase for lysine succinylation, malonylation, or glutarylation has not been identified yet, and investigation on the regulation of these three acidic lysine modifications has mainly been focusing on the deacylase sirtuin 5 (SIRT5) [10,21]. However, little is known about the biology that regulated by SIRT5. Phenotypical characterization conducted in *Sirt5* knockout (KO) mice reveals that these animals exhibit apparently normal size, body weight, food intake, mobility, and fertility under normal physiological conditions [22]. Of note, when exposed to 1-methyl-4-phenyl-1,2,3,6-tetrahydropyridine (MPTP), *Sirt5* KO mice display more severe nigrostriatal dopaminergic degeneration and accelerated motor deficit [23]. The dopaminergic neurotoxin MPTP blocks complex I (NADH-ubiquinone oxidoreductase) of the mitochondrial electron transport chain, generates ROS, and subsequently induces neuronal death [24,25], recapitulating the hallmarks of Parkinson's disease in humans [26]. Moreover, *Sirt5* KO mice exhibit a higher susceptibility to ischemia–reperfusion injury in the heart, which is associated with increased generation of ROS [27]. These findings point out that SIRT5 may preserve cellular antioxidant capacity, although the underlying mechanism still remains unclear. This study is directed toward understanding how SIRT5 regulates cellular redox status and susceptibility to oxidative damage. Our results uncover a previously unknown mechanism by which SIRT5 desuccinylates and deglutarylates IDH2 and G6PD, respectively, and activates both enzymes to maintain cellular NADPH homeostasis and redox potential during oxidative stress.

Results and Discussion

Sirt5 protects cells from oxidative damage

SIRT5 is a global regulator of lysine succinylation, malonylation, and glutarylation in mitochondria and can impact enzymes involved in diverse mitochondrial metabolic pathways [10,17–20]. To decipher the role of SIRT5 in regulating mitochondrial function, we investigated murine embryonic fibroblasts (MEFs) isolated from *Sirt5* wild-type (WT) and KO mice littermates. Western blot analysis demonstrated that as expected, the protein expression of Sirt5 was abolished in *Sirt5* KO MEFs (Fig EV1A). The effect of SIRT5 deficiency on overall mitochondrial function was evaluated by measuring the oxygen consumption rate (OCR), an indicator of oxidative phosphorylation, in the presence of a series of metabolic inhibitors and uncoupling agents (Fig EV1B and C). As shown, the basal oxygen consumption was significantly ($P < 0.001$) decreased by 26% in *Sirt5* KO MEFs compared to WT control cells. The rate of oligomycin-sensitive oxygen consumption, which reflects the amount of oxygen consumption linked to ATP production [28], was significantly ($P < 0.001$) decreased by 31% in *Sirt5* KO MEFs compared to WT control cells. After oligomycin, cells were treated with FCCP, which permeabilizes the inner mitochondrial membrane and induces maximal and uncoupled respiration [29,30]. The response to FCCP was also significantly ($P < 0.01$) lower in *Sirt5* KO MEFs than WT cells. These results suggest that SIRT5 is important for preserving normal respiratory capacity of mitochondrion.

Given that oxidative phosphorylation is one of the main sources for ROS production in mammalian cells [31], we determined ROS levels in *Sirt5* KO and WT MEFs. Surprisingly, we found that although oxidative phosphorylation is impaired in *Sirt5* KO MEFs, the ROS level was significantly ($P < 0.01$) increased by twofold in *Sirt5* KO MEFs compared to WT control cells (Fig 1A). Moreover, the ratios of [GSH/GSSG] and [NADPH/$NADP^+$] were reduced by 77% ($P < 0.05$) and 50% ($P < 0.001$), respectively, in *Sirt5* KO MEFs compared to WT control cells (Fig 1B and C). Furthermore, *Sirt5* KO MEFs displayed a significant ($P < 0.001$) reduction in cellular growth rate (Fig 1D). These MEFs also exhibited remarkably higher levels of cleaved PARP and caspase-3, two indicators of apoptosis, when subjected to paraquat (a toxin which impairs cellular redox cycling and induces ROS formation) (Fig 1E), and consequently, a significantly ($P < 0.01$) higher incidence of cell death upon paraquat treatment (Fig 1F). These results imply that SIRT5 regulates cellular redox status at least in part by modulating NADPH homeostasis in cultured cells.

Figure 1. Sirt5 protects cells from oxidative stress.

A *Sirt5* deficiency leads to higher ROS levels in MEFs. ROS levels were determined in the indicated MEFs as described in the Materials and Methods. The results are average ± SD of three independent experiments, $^{**}P < 0.01$ (two-tailed unpaired *t*-test).

B *Sirt5* deficiency suppresses GSH production in MEFs. The ratio of [GSH/GSSG] was determined in cell extracts as described in the Materials and Methods. The results are average ± SD of three independent experiments, $^{*}P < 0.05$ (two-tailed unpaired *t*-test).

C *Sirt5* deficiency inhibits NADPH production in MEFs. The ratio of [NADPH/$NADP^+$] was determined in cell extracts as described in the Materials and Methods. The results are average ± SD of three independent experiments, $^{***}P < 0.001$ (two-tailed unpaired *t*-test).

D *Sirt5* deficiency decreases cell growth. MEF cells were seeded in 6-well plates at a density of 50,000 cells/well, and cell growth rate was carefully monitored every 1–2 days by cell counting for 8 days. The results are average ± SD of three independent experiments, $^{*}P < 0.05$, $^{***}P < 0.001$ (two-tailed unpaired *t*-test).

E *Sirt5* deficiency leads to higher sensitivity of MEFs to paraquat. The levels of cleaved PARP and caspase-3 were determined by Western blot analysis.

F *Sirt5* protects MEFs from ROS-induced cell death. Wild-type and *Sirt5* KO MEFs were treated with paraquat (500 μM) for 24 h, and then, cell viability was determined by counting the remaining adherent cells. The results are average ± SD of three independent experiments, $^{**}P < 0.01$ (two-tailed unpaired *t*-test).

G–I *Sirt5* deficiency inhibits the production of NADPH and GSH and increases lipid peroxide in mouse brains after paraquat injection. Female *Sirt5* KO and WT littermates (n = 3–5 per group) were intraperitoneally injected with saline or paraquat (10 mg/kg) once a week for 3 consecutive weeks. The ratios of [NADPH/$NADP^+$] and [GSH/GSSG] and the level of lipid peroxide were determined in tissue extracts. The results are average ± SD. $^{*}P < 0.05$, n.s.: not significant (two-tailed unpaired *t*-test).

J, K *Sirt5* KO mice are more sensitive to paraquat-induced nigrostriatal dopaminergic degeneration. Female *Sirt5* KO and WT littermates were treated with paraquat as in (G–I). The brain sections were stained to detect tyrosine hydroxylase (TH)-positive dopaminergic neurons in the SNc region, as described in the Materials and Methods. Representative immunohistochemistry images (original magnification, 100×; scale bar, 100 μm) and the corresponding quantifications are shown in (J) and (K), respectively. The results are average ± SD. $^{*}P < 0.05$, n.s.: not significant (two-tailed unpaired *t*-test).

Source data are available online for this figure.

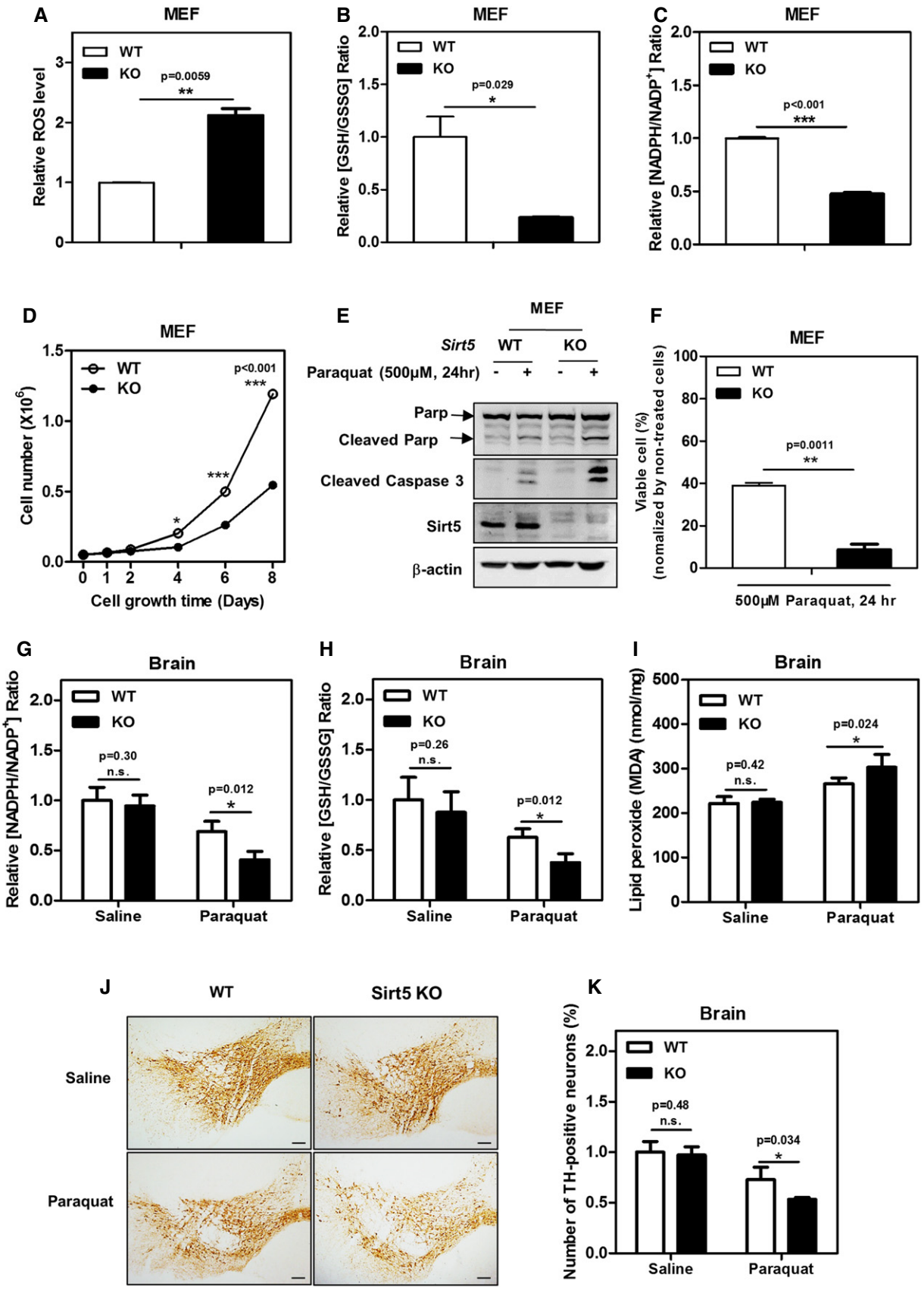
A
MEF
WT
KO
p=0.0059
**
Relative ROS level
B
MEF
WT
KO
p=0.029
*
Relative [GSH/GSSG] Ratio
C
MEF
WT
KO
p<0.001
***
Relative [NADPH/NADP+] Ratio
D
MEF
WT
KO
p<0.001
***
Cell number (X10^6)
Cell growth time (Days)
E
MEF
Sirt5 WT KO
Paraquat (500μM, 24hr) - + - +
Parp
Cleaved Parp
Cleaved Caspase 3
Sirt5
β-actin
F
MEF
WT
KO
p=0.0011
**
Viable cell (%)
(nomalized by non-treated cells)
500μM Paraquat, 24 hr
G
Brain
WT
KO
p=0.30
n.s.
p=0.012
*
Relative [NADPH/NADP+] Ratio
Saline
Paraquat
H
Brain
WT
KO
p=0.26
n.s.
p=0.012
*
Relative [GSH/GSSG] Ratio
Saline
Paraquat
I
Brain
WT
KO
p=0.42
n.s.
p=0.024
*
Lipid peroxide (MDA) (nmol/mg)
Saline
Paraquat
J
WT
Sirt5 KO
Saline
Paraquat
K
Brain
WT
KO
p=0.48
n.s.
p=0.034
*
Number of TH-positive neurons (%)
Saline
Paraquat

Figure 1.

Next, we compared the *in vivo* response of female *Sirt5* KO mice and WT littermates after paraquat injection. As shown, no significant difference in the [NADPH/NADP$^+$] or [GSH/GSSG] ratio was found in the brain of *Sirt5* KO and WT mice under non-stress condition (upon saline injection). However, the [NADPH/NADP$^+$] and [GSH/GSSG] ratios were significantly ($P < 0.05$) lower in the brain of *Sirt5* KO mice than WT controls under oxidative stress condition (upon paraquat challenge) (Fig 1G and H). In accord, the level of lipid peroxide (MDA) was significantly ($P < 0.05$) higher in the brain of *Sirt5* KO mice than WT controls after paraquat injection (Fig 1I). Moreover, *Sirt5* KO mice appear to be more sensitive to paraquat-induced nigrostriatal dopaminergic degeneration, as the number of tyrosine hydroxylase (TH)-positive dopaminergic neurons was significantly ($P < 0.05$) reduced in the substantia nigra pars compacta (SNc) region in the brain of *Sirt5* KO mice after paraquat injection (Fig 1J and K). These findings support a crucial role of SIRT5 in regulating NADPH homeostasis and the redox status *in vivo*.

SIRT5 preserves cellular antioxidant capacity partially through activating NADPH-producing G6PD and IDH2

To check whether SIRT5 could regulate cellular redox status in other cell types besides MEFs, we generated stable HEK293T cells with *SIRT5* knockdown by retrovirus infection (Fig EV2A). *SIRT5* knockdown significantly ($P < 0.01$) reduced the [NADPH/NADP$^+$] ratio by as much as 36%, reaffirming that SIRT5 is an important contributor to NADPH pools in the cell (Fig 2A). The lower [NADPH/NADP$^+$] ratio is in line with the lower [GSH/GSSG] ratio and higher ROS in *SIRT5* knockdown cells (Fig 2B and C). Moreover, *SIRT5* knockdown cells exhibited higher levels of cleaved PARP and caspase-3 as well as a higher incidence of cell death when subjected to paraquat (Fig 2D and E). Notably, the sensitivity to paraquat-induced cell death positively correlated with the *SIRT5* knockdown efficiency, as shRNA #2 was more potent in both *SIRT5* knockdown and changing the redox parameters (i.e., [GSH/GSSG] ratio, [NADPH/NADP$^+$] ratio, and ROS) than shRNA #1. Collectively, these findings further support an important role of SIRT5 in controlling NADPH homeostasis and protecting cells from oxidative damage.

To determine which NADPH-producing enzyme(s) may contribute to the observed redox imbalance in *SIRT5* knockdown cells, we measured the activity of NADPH-producing enzymes, including G6PD, 6PGD, ME1, MTHFD1/2, and IDH1/2 in *SIRT5* knockdown HEK293T cells (Fig 2F). Our data demonstrated that the activities of endogenous G6PD/6PGD and IDH1/2, but not ME1 and MTHFD1/2, were substantially reduced in *SIRT5* knockdown cells and that the reduction in enzyme activity of G6PD/6PGD or IDH1/2 was positively correlated with the *SIRT5* knockdown efficiency in these cells (Fig 2G). *SIRT5* knockdown reduced activities of endogenous G6PD and IDH2 without changing their protein levels in HEK293T cells (Fig EV2B), indicating that the inhibitory effect of *SIRT5* depletion on G6PD and IDH2 is most likely to be posttranslational. To test whether SIRT5 directly regulate the activity of NADPH-producing enzymes, we next expressed Flag-tagged protein of G6PD, 6PGD, ME1, MTHFD1, MTHFD2, IDH1, or IDH2 in HEK293T cells, immunoprecipitated with Flag beads, eluted by Flag peptides, and then incubated each protein with His-tagged SIRT5 *in vitro*. Interestingly, our data demonstrated that the activities of G6PD and IDH2, but not the other enzymes, were significantly increased when co-incubated with SIRT5 (Fig 2H). Taken together, these results suggest that SIRT5 modulates cellular NADPH homeostasis and protects cells from oxidative stress at least in part by maintaining the activity of G6PD and IDH2.

SIRT5 promotes IDH2 desuccinylation and G6PD deglutarylation to activate these two enzymes and maintain NADPH homeostasis

Previous proteomic studies have identified a large number of succinylated, malonylated, and glutarylated proteins [10,17–20]. Among these identified acylated proteins are several NADPH-producing metabolic enzymes, including human G6PD and IDH2 as well as mouse Idh2 (Fig EV3). It has previously been reported that succinyl-CoA can lead to nonenzymatic succinylation of lysine residues in proteins [32]. As expected, when immunoprecipitated Flag-tagged G6PD or IDH2 was incubated with succinyl-CoA *in vitro*, lysine succinylation of each protein was dramatically increased (Fig 3A and B). Succinyl-CoA incubation significantly ($P < 0.05$) decreased the activity of Flag-IDH2, while the activity of Flag-G6PD was largely unaffected (Fig 3A and B), suggesting that succinylation

Figure 2. SIRT5 preserves cellular antioxidant capacity partially through activating NADPH-producing G6PD and IDH2.

A Knockdown of *SIRT5* inhibits NADPH production in HEK293T cells. The ratio of [NADPH/NADP$^+$] was determined in cell extracts as described in the Materials and Methods. The results are average ± SD of three independent experiments, $^{**}P < 0.01$, $^{***}P < 0.001$ (two-tailed unpaired *t*-test).

B Knockdown of *SIRT5* suppresses GSH production in HEK293T cells. The ratio of [GSH/GSSG] was determined in cell extracts as described in the Materials and Methods. The results are average ± SD of three independent experiments, $^{**}P < 0.01$ (two-tailed unpaired *t*-test).

C Knockdown of *SIRT5* leads to higher ROS levels in HEK293T cells. ROS levels were determined in the indicated stable cells as described in the Materials and Methods. The results are average ± SD of three independent experiments, $^{***}P < 0.001$ (two-tailed unpaired *t*-test).

D Knockdown of *SIRT5* leads to higher sensitivity to paraquat. The expression levels of PARP and caspase-3 were determined by Western blot analysis.

E SIRT5 protects HEK293T cells from ROS-induced cell death. The indicated stable HEK293T cells were treated as mentioned in (D), and then, cell viability was determined by counting the remaining adherent cells. The results are average ± SD of three independent experiments, $^{**}P < 0.01$ (two-tailed unpaired *t*-test).

F Cartoon representation of major NADPH-producing enzymes in the cell. As shown, G6PD, 6PGD, ME1, IDH1, and MTHFD1 are located in the cytosol, while IDH2 and MTHFD2 are located in mitochondria.

G The activities of G6PD/6PGD and IDH1/2 are reduced in stable HEK293T cells with *SIRT5* knockdown. Activities of the indicated endogenous proteins were determined in cell extracts as described in the Materials and Methods. The results are average ± SD of three independent experiments, $^{*}P < 0.05$, $^{**}P < 0.01$, $^{***}P < 0.001$, n.s.: not significant (two-tailed unpaired *t*-test).

H G6PD and IDH2 are activated by SIRT5 *in vitro*. Upon pre-incubation with SIRT5 *in vitro*, the activities of the indicated ectopically expressed proteins were determined as described in the Materials and Methods. The results are average ± SD of three independent experiments, $^{**}P < 0.01$, n.s.: not significant (two-tailed unpaired *t*-test).

Source data are available online for this figure.

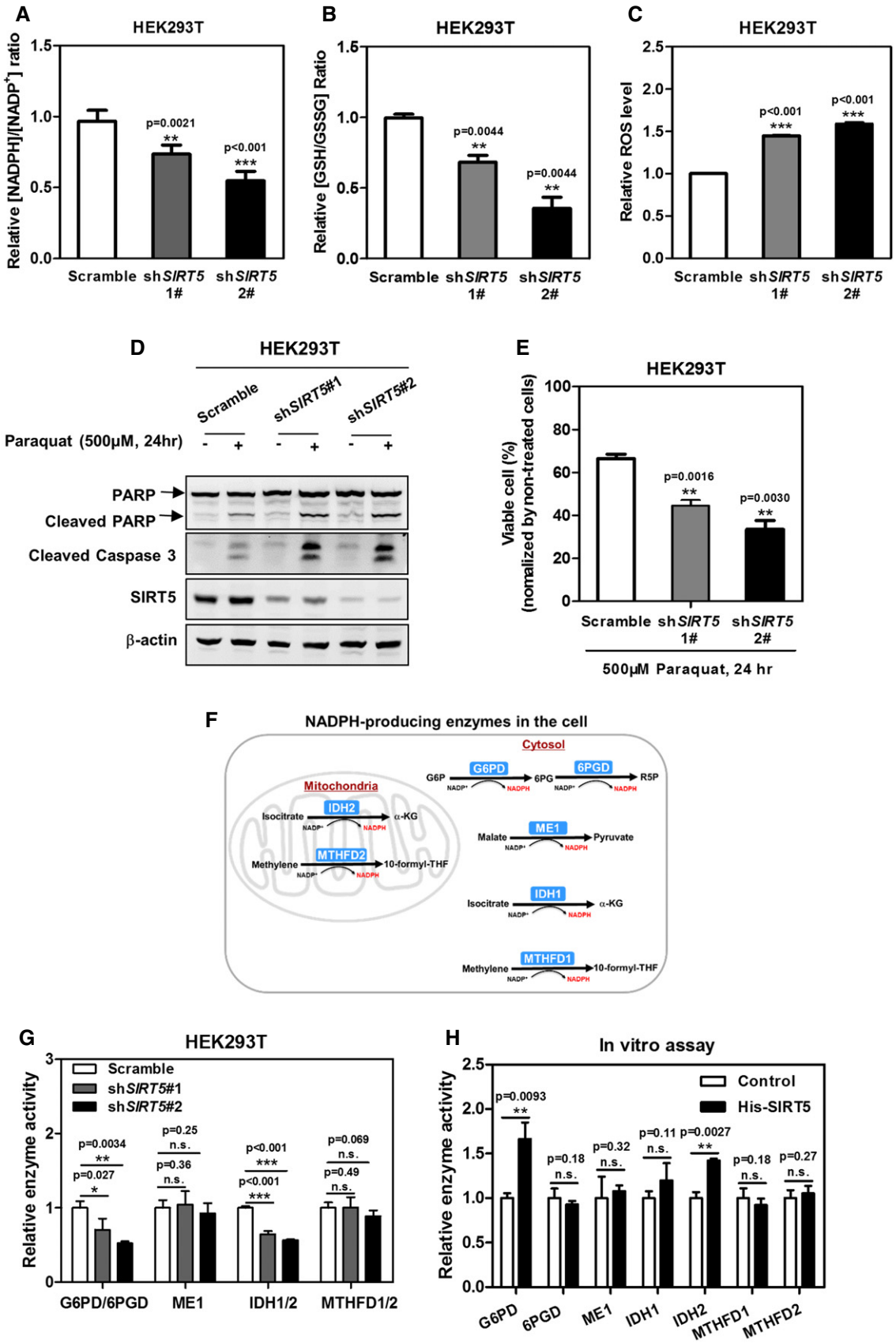

Figure 2.

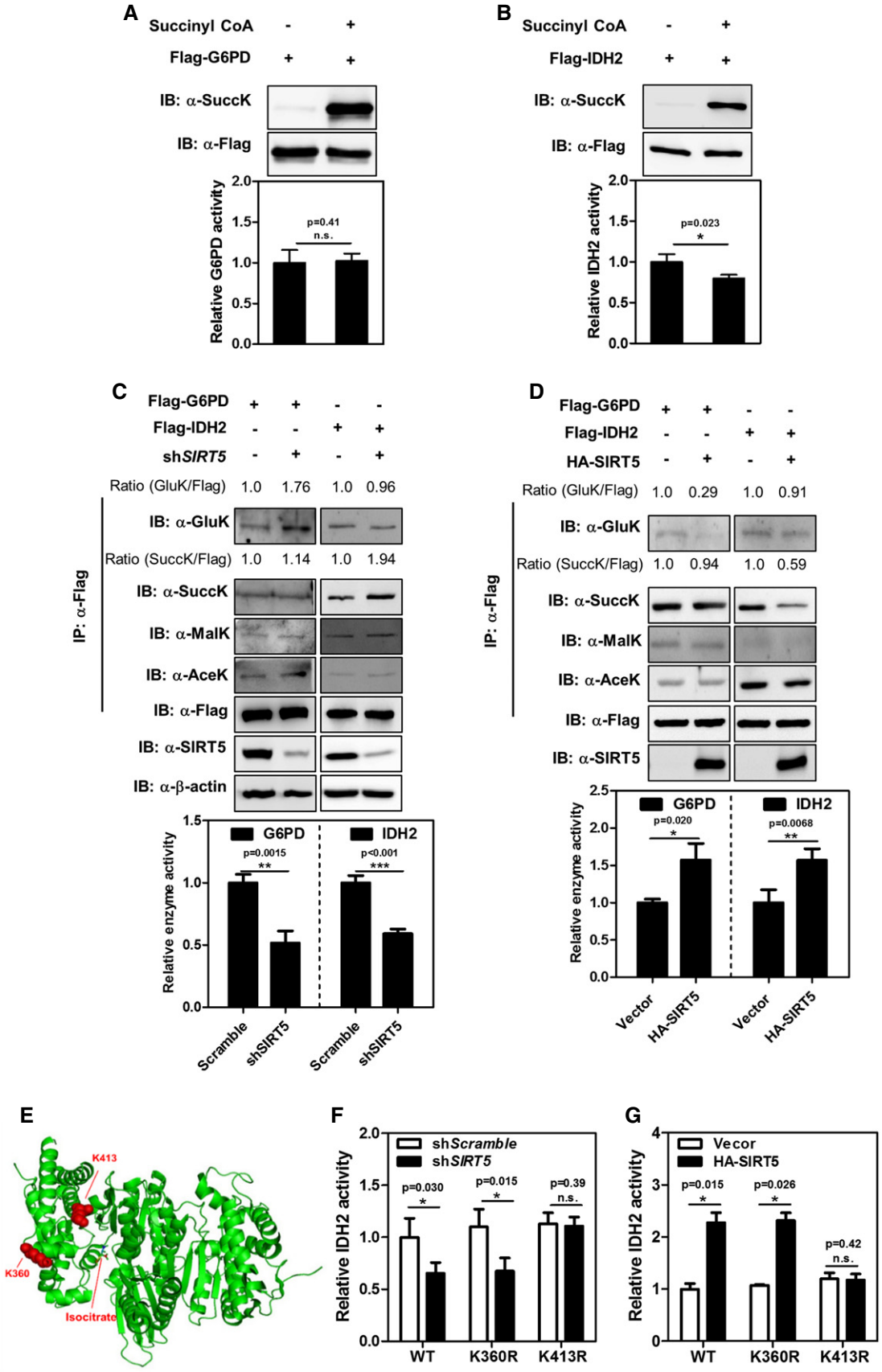

Figure 3.

Figure 3. SIRT5 promotes IDH2 desuccinylation and G6PD deglutarylation to activate these two enzymes and maintain NADPH homeostasis.

A G6PD activity is not regulated by lysine succinylation. Purified Flag-tagged G6PD was incubated with or without succinyl-CoA (1 mM) at 30°C for 15 min, followed by measurement of G6PD enzyme activity as described in the Materials and Methods. The results are average ± SD of three independent experiments. n.s.: not significant (two-tailed unpaired *t*-test).

B IDH2 activity is suppressed by lysine succinylation. Purified Flag-tagged IDH2 was incubated with or without succinyl-CoA (1 mM) at 30°C for 15 min, followed by measurement of IDH2 enzyme activity as described in the Materials and Methods. The results are average ± SD of three independent experiments, $*P < 0.05$ (two-tailed unpaired *t*-test).

C *SIRT5* knockdown increases G6PD glutarylation and IDH2 succinylation, respectively, and decreases both enzyme activities. Flag-G6PD or Flag-IDH2 was ectopically expressed in the indicated stable HEK293T cells. G6PD/IDH2 proteins were purified by immunoprecipitated with Flag beads and eluted with Flag peptide, followed by determination of their lysine modifications and enzyme activity. The results are average ± SD of three independent experiments, $**P < 0.01$, $***P < 0.001$ (two-tailed unpaired *t*-test).

D SIRT5 decreases G6PD glutarylation and IDH2 succinylation and increases both enzyme activities. Flag-G6PD or Flag-IDH2 was co-overexpressed with HA-SIRT5 in HEK293T cells. G6PD and IDH2 proteins were purified by immunoprecipitation with Flag beads and eluted with Flag peptide, followed by determination of their lysine modifications and enzyme activity. The results are average ± SD of three independent experiments, $*P < 0.05$, $**P < 0.01$ (two-tailed unpaired *t*-test).

E Cartoon representation of porcine mitochondrial IDH2 structure shows isocitrate binding pocket (PDB ID: 1LWD) [33], made by Pymol (www.pymol.org). The protein is colored in light green and isocitrate in rainbow, with Lys360 and Lys413 residues in IDH2 being colored in red.

F, G K413 in IDH2 may be a key succinylation site that is directly targeted by SIRT5. The indicated Flag-tagged IDH2 proteins were overexpressed in HEK293T cells with stable *SIRT5* knockdown or SIRT5 co-overexpression. Wild-type and mutant IDH2 proteins were purified by Flag beads and eluted with Flag peptide, followed by measurement of IDH2 enzyme activity. The results are average ± SD of three independent experiments, $*P < 0.05$, n.s.: not significant (two-tailed unpaired *t*-test).

Source data are available online for this figure.

may negatively regulate IDH2, but not G6PD. Supporting this notion, the succinylation level of Flag-IDH2 was increased, while IDH2 enzyme activity was significantly ($P < 0.001$) decreased by 41% in *SIRT5* knockdown HEK293T cells (Fig 3C). On the other hand, co-overexpression of Flag-IDH2 with HA-SIRT5 decreased IDH2 succinylation, but significantly increased IDH2 enzyme activity ($P < 0.01$, increased by ~1.6-fold) (Fig 3D). Moreover, depletion of endogenous *SIRT5* or co-overexpression of HA-SIRT5 did not affect lysine glutarylation, malonylation, and acetylation of Flag-IDH2 (Fig 3C and D). These findings suggest that SIRT5 regulates IDH2 activity by controlling IDH2 succinylation.

There are 17 different lysine residues in IDH2 which can potentially be modified by succinylation [17,18,20]. Among these, several sites seem to be highly targeted by SIRT5, including K80, K155, K263, K360, and K413. Based on the crystal structure [33], two lysine sites, K360 and K413, which are adjacent to the substrate binding site, imply that succinylation of these two residues might compromise the binding pocket for isocitrate and inhibit IDH2 activity (Fig 3E). To test this hypothesis, we mutated each of these two putative succinylation sites to arginine (R). The K to R mutation retains a positive charge and is often used as a desuccinylated mimetic. We found that, like wild-type IDH2, the activity of K360R mutant IDH2 was decreased by *SIRT5* knockdown and was increased by SIRT5 overexpression (Fig 3F and G). Interestingly, K413R mutant IDH2 displayed a negligible response to either *SIRT5* knockdown or SIRT5 overexpression in changing enzyme activity (Fig 3F and G), suggesting that K413 in IDH2 may be a key succinylation site that is directly targeted by SIRT5.

Moreover, our data demonstrated that the glutarylation level of Flag-G6PD was increased in HEK293T cells with *SIRT5* knockdown, which may contribute to a significant reduction in G6PD enzyme activity ($P < 0.01$, decreased by 48%) (Fig 3C). On the other hand, co-overexpression of Flag-G6PD with HA-SIRT5 led to a reduction in G6PD glutarylation and a concomitant increase in G6PD enzyme activity ($P < 0.05$, increased by ~1.6-fold) (Fig 3D). Lysine succinylation, malonylation, and acetylation levels of Flag-G6PD were largely unaffected by either *SIRT5* knockdown or SIRT5 co-overexpression (Fig 3C and D). Collectively, these findings suggest that SIRT5 regulates G6PD activity by controlling G6PD glutarylation.

SIRT5 desuccinylase activity is triggered by oxidative stimuli

Finally, we investigated whether oxidative stress alters SIRT5 expression or enzymatic activity. Western blotting and quantitative RT–PCR showed that paraquat or H_2O_2 treatment had no effect on the mRNA or protein expression of SIRT5 (Fig 4A and B). Furthermore, we observed that paraquat or H_2O_2 dose-dependently activated the desuccinylase activity of SIRT5 (Fig 4C and D). *In vitro* incubation of purified SIRT5 protein with either paraquat or H_2O_2 did not affect the desuccinylase activity of SIRT5 (Fig 4C and E), suggesting that the increased SIRT5 activity is not due to a direct oxidation of SIRT5 by the oxidants. However, treatment of the Flag-SIRT5 expressing HEK293T cells with paraquat or H_2O_2 did increase the ability of SIRT5 to activate IDH2 (Fig 4F). Together, our data indicate that oxidative stress can increase the desuccinylase activity of cellular SIRT5.

Aging is a universal phenomenon observed in all organisms, which is characterized by a progressive decline in organ functions. The free radical theory of aging states that the process of aging is at least partly due to the accumulation of oxidative damage caused by ROS [34]. Indeed, numerous studies have provided evidence to support it. For instance, *C. elegans* mutations that have enhanced oxidative defense extend lifespan, whereas shorter lifespan mutations are more sensitive to free radicals [35,36]. Interesting, overexpression of catalase targeted to mitochondria leads to extension of life span in mice, while catalase targeted to nucleus and peroxisome have little effect [37]. One explanation is that catalase catalyzes the decomposition of hydrogen peroxide to water and oxygen, and mitochondria are thought to be the major cellular source of ROS. To prevent from ROS-induced damage, cells have developed antioxidant defense systems to balance the antioxidant defenses and ROS production during aging [38]. The redox balance is maintained in part by ratios of some redox couples, such as the [GSH/GSSG] and [NADPH/$NADP^+$] ratios. NADPH is commonly required for the generation of GSH [39], which scavenges ROS and plays a critical

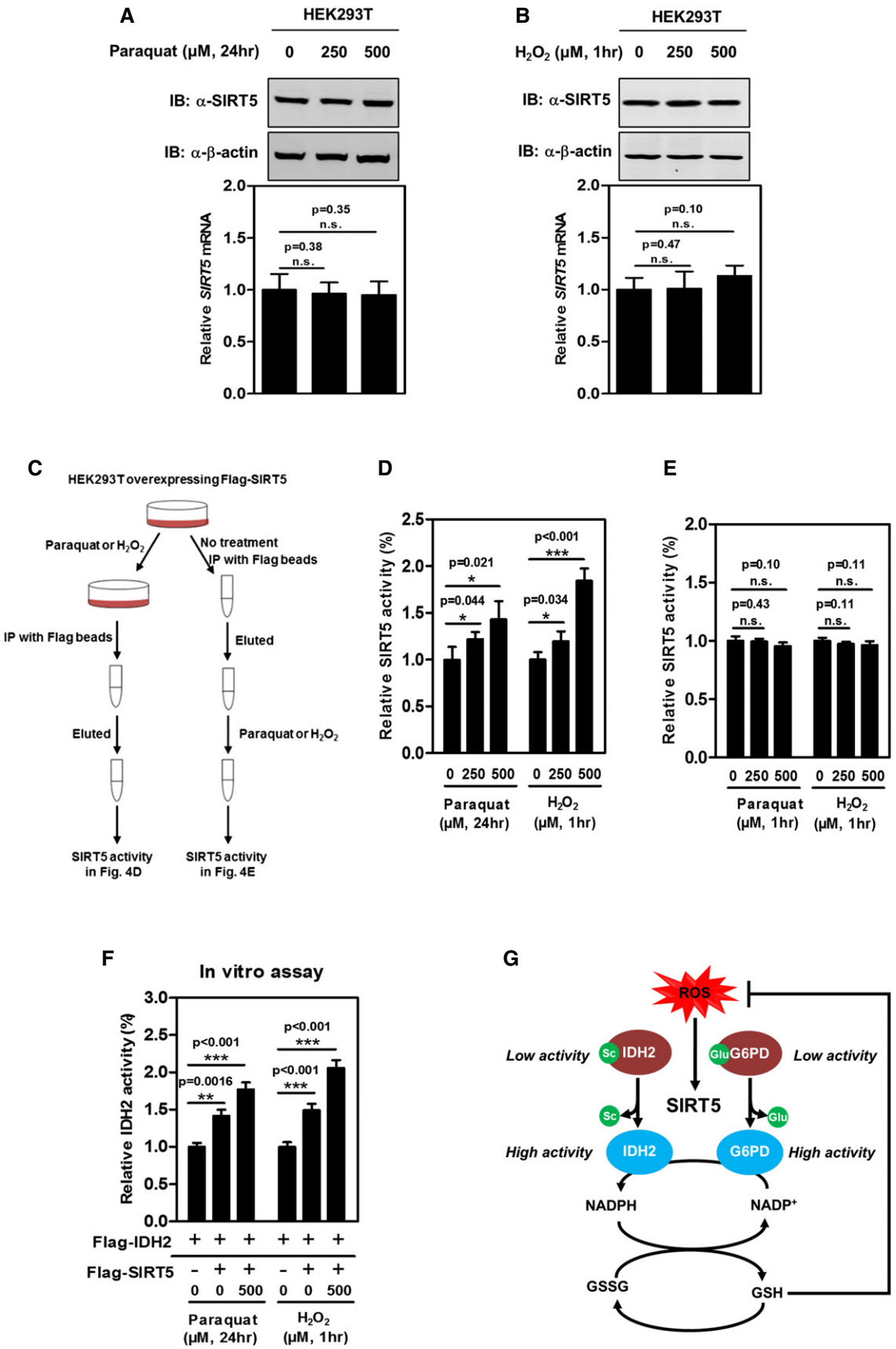

Figure 4.

Figure 4. SIRT5 desuccinylase activity, but not its expression, is regulated by oxidative stimuli.

A, B SIRT5 expression is not affected by chemical oxidant treatment. HEK293T cells were treated with paraquat (A) or H_2O_2 (B) for the indicated periods. The mRNA and protein expressions of endogenous SIRT5 were determined by quantitative real-time PCR and Western blot analysis, respectively. The results are average ± SD of three independent experiments. n.s.: not significant (two-tailed unpaired *t*-test).

C Schematic representation of the experimental workflow for (D) and (E).

D The desuccinylase activity of SIRT5 is stimulated by oxidative stimuli. Flag-SIRT5 was ectopically expressed in HEK293T cells. The transfected cells were treated with increasing concentrations of paraquat or H_2O_2 for the indicated periods. Flag-SIRT5 was purified by immunoprecipitation with Flag beads, eluted with Flag peptide, and then subjected to the desuccinylase activity assay as described in the Materials and Methods. The SIRT5 desuccinylase activity was normalized against its protein level. The results are average ± SD of three independent experiments, $*P < 0.05$, $***P < 0.001$ (two-tailed unpaired *t*-test).

E *In vitro* incubation with chemical oxidants does not affect the desuccinylase activity of SIRT5. Flag-tagged SIRT5 was ectopically expressed in HEK293T cells and then purified by immunoprecipitation with Flag beads and eluted with Flag peptide. The purified Flag-SIRT5 was treated with increasing concentrations of paraquat or H_2O_2 at room temperature for 1 h and then subjected to the desuccinylase activity assay as described in the Materials and Methods. The SIRT5 desuccinylase activity was normalized against its protein level. The results are average ± SD of three independent experiments. n.s.: not significant (two-tailed unpaired *t*-test).

F Chemical oxidants enhance the ability of SIRT5 to activate IDH2. Flag-SIRT5 was ectopically expressed in HEK293T cells, and the transfected cells were treated with increasing concentrations of paraquat or H_2O_2 for the indicated periods. Flag-SIRT5 was purified by immunoprecipitation with Flag beads, eluted with Flag peptide, and then incubated with purified Flag-IDH2 *in vitro*. IDH2 enzyme activity was measured as described in the Materials and Methods, normalized by its protein level. The results are average ± SD of three independent experiments, $**P < 0.01$, $***P < 0.001$ (two-tailed unpaired *t*-test).

G A proposed model for a role of SIRT5 in mediating oxidative stress to increase IDH2 and G6PD activities, NADPH production, and cellular protection. SIRT5 is activated by oxidative stress by a yet unknown mechanism. The active SIRT5 stimulates IDH2 and G6PD by desuccinylation and deglutarylation, respectively, thereby increasing NADPH production and protecting cells from ROS damage.

Source data are available online for this figure.

role in oxidative stress resistance. In addition, NADPH is also used mostly as a reducing agent in anabolic pathways, such as lipid synthesis, cholesterol synthesis, and fatty acid chain elongation. Hence, maintaining cellular NADPH homeostasis is important for a wide range of cellular processes.

Emerging evidence suggests that *SIRT5* is a candidate longevity gene as well as a risk factor for mitochondrial dysfunction-related disease, such as Parkinson's disease [40]. Moreover, SIRT5 deficiency decreases the expression of manganese superoxide dismutase (SOD2), a mitochondria-specific antioxidant enzyme, and exacerbates nigrostriatal dopaminergic degeneration caused by MPTP in mice [23]. These findings imply a potential role of SIRT5 in cellular protection from oxidative stress. In this study, we found that *Sirt5* KO MEFs display higher ROS level and revealed a possible mechanism involving posttranslational inactivation of IDH2 and G6PD. It is known that endogenous ROS can be produced by multiple sources, including the respiratory chain and oxidative phosphorylation in the mitochondrion, the NADPH oxidase in the plasma membrane, and the endoplasmic reticulum and peroxisomes. Apparently, the observed higher ROS in Sirt5-defective MEFs is not derived from mitochondrial respiration and the OXPHOS pathway, as the oxygen consumption rates were lower in *Sirt5* KO MEFs than WT cells. In addition to ROS production, ROS scavenging is also crucial to balance the redox state in the cell. It is acknowledged that cellular detoxification of, or protection against, harmful ROS commonly requires NADPH-dependent reducing equivalents (*e.g.*, GSH). We show in the current study that SIRT5 preserves cellular antioxidant capacity partially by modulating the activity of NADPH-producing enzymes, IDH2 and G6PD. Our study provides both biochemical and cellular evidence demonstrating K413 in IDH2 may be a key succinylation site that is directly targeted by SIRT5. Nevertheless, our data cannot exclude the possibility that K413R mutation may alter IDH2 conformation in a way that the mutant enzyme cannot be regulated by succinylation and thus is insensitive to SIRT5. To date, no glutarylated lysine site(s) in G6PD has been identified by proteomic studies. Therefore, the mechanism for SIRT5 regulating G6PD glutarylation and activity still needs further investigation. Of interest, our data show that paraquat or H_2O_2 dose-dependently activates the desuccinylase activity of SIRT5, with no effect on the mRNA or protein levels of SIRT5. Future exploration will be needed to illuminate how these chemical oxidants increase SIRT5 enzyme activity.

In summary, our findings provide direct evidence showing that SIRT5 plays an important role in mediating oxidative stress to desuccinylate and deglutarylate IDH2 and G6PD, respectively, thereby activating both metabolic enzymes and maintaining cellular NADPH homeostasis and redox balance to protect against oxidative damage.

Materials and Methods

Antibodies

Antibodies specific to SIRT5 (Cell Signaling Technology, #8782), PARP (Cell Signaling Technology, #9532), caspase-3 (Cell Signaling Technology, #9665), pan-succinyl-lysine (PTM-401), pan-malonyl-lysine (PTM-901), pan-glutaryl-lysine (PTM-1151), pan-acetyl-lysine (Cell Signaling Technology, # 9441), HA (Santa Cruz, sc-7392), and Flag (Shanghai Genomics, 4110-20) were purchased commercially.

Plasmids

The cDNA encoding full-length human SIRT5, G6PD, 6PGD, ME1, IDH1, IDH2, MTHFD1, and MTHFD2 were cloned into Flag- or HA-tagged vectors (pcDNA-Flag; pcDNA-HA). Point (Site) mutations of IDH2 were generated by QuikChange Site-Directed Mutagenesis kit (Stratagene).

Cell culture, transfection, and treatment

Both HEK293T cells and mouse embryonic fibroblasts (MEFs) were cultured in Dulbecco's modified Eagle's medium (DMEM, Gibco) supplemented with 10% fetal bovine serum (Gibco) and antibiotics

(100 units/ml penicillin and 100 μg/ml streptomycin), in 5% CO_2 atmosphere at 37°C.

Plasmid transfection was carried out using the polyethyleneimine (PEI, Sigma-Aldrich) or lipofectamine 2000 (Invitrogen).

Oxidative agents, H_2O_2 (Sinopharm) and paraquat (Sigma-Aldrich), were used to induce oxidative stress.

Immunoprecipitation and Western blotting

For Flag immunoprecipitations, cells were lysed in an ice-cold NP-40 buffer [50 mM Tris–HCl (pH 7.4), 150 mM NaCl, 0.1% NP-40, and protease inhibitors]. Cell lysate was incubated with anti-Flag M2 affinity resin (Sigma-Aldrich, A2220) for 3 h at 4°C, washed three times with ice-cold NP-40 buffer, and analyzed by SDS–PAGE and immunoblotting. Western blot analysis was carried out according to standard methods.

Measurement of intracellular ROS

Intracellular ROS production was determined by using a fluorescent dye 2′, 7′-dichlorofluorescein diacetate (H_2DCF-DA, Sigma-Aldrich). Briefly, cells were washed with PBS and incubated with 10 μM H_2DCF-DA at 37°C for 30 min to load the fluorescent dye. Cells were washed twice with PBS and trypsinized for menadione treatments. Fluorescence (Ex.488 nm, Em.525 nm) was monitored by a SpectraMax M5 Microplate Reader (Molecular Devices).

Measurement of intracellular GSSG and GSH

Intracellular GSSG and GSH levels were determined by using liquid chromatography–mass spectrometry (LC-MS/MS). In short, cells were harvested in 80% (v/v) pre-cold (−80°C) methanol and centrifuged at 4°C at 15,000 *g* for 15 min. The supernatants were then subjected to LC-MS analysis using a ShimazuLC (LC-20AB pump) system coupled with 4000 QTrap triple quadrupole mass spectrometer (AB sciex). A Phenomenex NH2 column (50 mm × 2.0 mm I.D., 5-μm particle size, 100 Å) was used. The mass spectrometer was optimized and set up in selected reaction monitoring (SRM) scan mode for monitoring the [M-H] of GSSG (*m/z* 611.6/306.2) and GSH (*m/z* 306.2/142.8). The Analyst Software was used for analysis.

Measurement of intracellular NADPH and NADP$^+$

The intracellular levels of NADPH and $NADP^+$ were measured by enzymatic cycling methods as previously described [41,42]. In brief, 1.5×10^6 cells were seeded in a 10-cm dish, and cells were lysed in 400 μl of extraction buffer (20 mM NAM, 20 mM $NaHCO_3$, 100 mM Na_2CO_3) and centrifuged at 1,200 × *g* for 15 min after 24 h. For NADPH extraction, 150 μl of the supernatant was incubated for 30 min at 60°C; 160 μl of NADP-cycling buffer (100 mM Tris–HCl, pH 8.0; 0.5 mM thiazolyl blue; 2 mM phenazine ethosulfate; 5 mM EDTA) containing 1.3 U of G6PD was added to a 96-well plate containing 20 μl of the cell extract. After incubation for 1 min at 30°C in darkness, 20 μl of 10 mM G6P was added to the mixture, and the change in absorbance at 570 nm was measured every 30 sec for 10 min at 30°C in a SpectraMax M5 Microplate Reader (Molecular Devices). All the samples were run in triplicate. The concentration of $NADP^+$ was calculated by subtracting NADPH (heated sample) from the total of $NADP^+$ and NADPH (unheated sample).

Cell survival assay

Murine embryonic fibroblasts were seeded in 6-well plates at a density of 50,000 cells/well, and cell numbers were counted every 1–2 days over a 8-day period by using Countstar IC1000. Moreover, stable HEK293T cells were seeded in 6-well plates at a density of 4×10^4 cells/well. After incubation with 500 μM paraquat (Sigma-Aldrich) for 24 h, the remaining living cells were trypsinized and counted by Countstar IC1000.

Animal experiments

Sirt5 KO mice (129-strain background) were purchased from the Jackson Laboratory. These animals were backcrossed for four generations onto the C57BL/6J background. Animals were given unrestricted access to a standard diet and tap water. Animal experiments were performed at Fudan Animal Center in accordance with the animal welfare guidelines.

Paraquat injection and brain tissue preparation

Female Sirt5 KO mice and WT littermates (~12 weeks of age) were intraperitoneally injected with paraquat (10 mg/kg, Sigma-Aldrich) once a week for 3 consecutive weeks. Meanwhile, an equivalent volume of saline was injected into the control groups. At 3 weeks after injection, the animals were anesthetized with chloral hydrate (500 mg/kg) and perfused with 0.1 M PBS (pH 7.4), fixed by 4% paraformaldehyde (Sigma-Aldrich) in 0.1 M PBS (pH 7.4). Mouse brains were removed from the skull immediately after perfusion, post-fixed overnight in 4% paraformaldehyde at 4°C, and dehydrated with 20% and 30% sucrose dissolved in PBS. Thereafter, frozen sections were cut at 30 μm in coronal planes by using a freezing microtome (Leica Microsystems, Wetzlar, Germany) and were then collected in 0.1 M PBS (pH 7.4) for further analysis.

Immunohistochemistry (IHC) analysis

Stored free-floating sections were washed in PBS for 15 min for three times and treated for 30 min in 3% H_2O_2 to quench endogenous peroxidase activity. After washing, the sections were blocked in 5% normal goat serum (Vector Laboratories) and 0.3% Triton X-100 in PBS for 1 h at room temperature. The sections were then incubated overnight at 4°C with a tyrosine hydroxylase antibody (Merck Millipore, AB152) followed by a biotinylated goat anti-rabbit IgG antibody (Vector Laboratories), and ABC solution (Vector Laboratories). After washing in PBS, the sections were visualized using DAB, washed in PBS, mounted on gelatin-coated slides, and air-dried overnight. Finally, sections were dehydrated in alcohol, cleared in xylene, and permanently mounted.

NADPH-producing enzyme activity assay

Flag-tagged enzymes were overexpressed in HEK293T cells, immunoprecipitated, and eluted by 250 mg/ml Flag peptide (Gilson Biochemical). Reactions were started by adding enzymes into the

assay buffer: G6PD and 6PGD activity assay buffer: 50 mM Tris–HCl (pH 7.6), 0.1 mM $NADP^+$, 0.2 mM glucose-6-phosphate (G6P), or 0.2 mM 6-phosphogluconate; ME1 activity assay buffer: 50 mM Tris–HCl (pH 7.6), 1 mM $MgCl_2$, 0.5 mM $NADP^+$, and 40 mM malate; IDH1/2 activity assay buffer: 100 mM potassium phosphate, 5 mM $MgCl_2$, 0.25 mM $NADP^+$, and 2.5 mM isocitrate; and MTHFD1/2 activity assay buffer: 2 mM potassium phosphate, 36 mM 2-mercaptoethanol, 25 mM 3-morpholinopropanesulfonate, 250 mM NADPH, and 200 μM formyl H4folate. The change in NADPH fluorescence (Ex. 350 nm, Em.470 nm) was monitored by a fluorescence spectrophotometer (HITACHI F-4600).

In vitro enzyme assay

Flag-tagged NADPH-producing enzymes were immunoprecipitated with anti-Flag M2 affinity resin (Sigma-Aldrich) and eluted with Flag peptide. The eluted proteins were incubated with His-SIRT5 (Sigma-Aldrich) in 25 mM Tris–HCl (pH 7.5), 1 mM $MgCl_2$, 1 mM DTT, 10% glycerol, and 1 mM NAD^+ for 1 h at 37°C and then subjected to the enzymatic activity assay and Western blot analysis.

RNA isolation and quantitative real-time PCR

Total RNA was isolated by TRIzol reagent according to the manufacturer instructions (Invitrogen). RNA was reverse-transcribed with oligo-dT primers and preceded to real-time PCR with gene-specific primers in the presence of SYBR Premix Ex Taq (TaKaRa). β-actin was used as endogenous controls. Primers sequences (5′–3′):
β-actin-forward: GCACAGAGCCTCGCCTT;
β-actin-reverse: GTTGTCGACGACGAGCG;
SIRT5-forward: GCACAGAGCCTCGCCTT;
SIRT5-reverse: GTTGTCGACGACGAGCG.

SIRT5 desuccinylase activity assay

SIRT5 desuccinylase activity was determined by using a commercially available SIRT5 activity assay kit (Enzo Life, BML-AK513-0001). Briefly, immunoprecipitated samples were incubated with Fluor de Lys®-succinyl, NAD^+, and the assay buffer at 37°C for 60 min. Once incubation was completed, developer and nicotinamide were added and incubated at room temperature for 10 min. Fluorescence (Ex.450 nm, Em.350 nm) was monitored by a SpectraMax M5 Microplate Reader (Molecular Devices).

Statistics

Statistical analyses were performed with a two-tailed unpaired Student's *t*-test. All data shown represent the results obtained from triplicated independent experiments with standard errors of the mean (mean ± SD). The values of $P < 0.05$ were considered statistically significant.

Expanded View for this article is available online.

Acknowledgements
We thank the members of the Fudan MCB laboratory for discussions and support throughout this study. This work was supported by the 973 Program (No. 2012CB910303 to D.Y.; No. 2012CB910101 to K.L.G.; No. 2013CB910502 to HXY.), the NSFC grant (No. 81372198 and No. 81522033 to D. Y. No. 81201534 and No. 81472566 to HXY), the NSFC Program of International Cooperation and Exchanges (No. 81120108016 to LXQ, Y.X.), and the Shanghai "Phosphor" Science Foundation, China (No. 14QA1400600 to D.Y.). This work was also supported by NIH grants (GM067113 and CA1638311 to Y.X.; CA196878 and GM51586 to K.L.G.).

Author contributions
LZ, FW, HY, and DY conceived the general framework of this study. LZ and FW designed experiments. LZ, FW, RS, XC, MZ, QX, YW, and SW performed experiments. LZ, FW, YX, K-LG, PY, HY, and DY prepared the manuscript.

Conflict of interest
The authors declare that they have no conflict of interest.

References

1. Margis R, Dunand C, Teixeira FK, Margis-Pinheiro M (2008) Glutathione peroxidase family – an evolutionary overview. *FEBS J* 275: 3959–3970
2. Kim SY, Lee SM, Tak JK, Choi KS, Kwon TK, Park JW (2007) Regulation of singlet oxygen-induced apoptosis by cytosolic $NADP^+$-dependent isocitrate dehydrogenase. *Mol Cell Biochem* 302: 27–34
3. Xu W, Yang H, Liu Y, Yang Y, Wang P, Kim SH, Ito S, Yang C, Wang P, Xiao MT *et al* (2011) Oncometabolite 2-hydroxyglutarate is a competitive inhibitor of alpha-ketoglutarate-dependent dioxygenases. *Cancer Cell* 19: 17–30
4. Choudhary C, Kumar C, Gnad F, Nielsen ML, Rehman M, Walther TC, Olsen JV, Mann M (2009) Lysine acetylation targets protein complexes and co-regulates major cellular functions. *Science* 325: 834–840
5. Kim SC, Sprung R, Chen Y, Xu Y, Ball H, Pei J, Cheng T, Kho Y, Xiao H, Xiao L *et al* (2006) Substrate and functional diversity of lysine acetylation revealed by a proteomics survey. *Mol Cell* 23: 607–618
6. Zhao S, Xu W, Jiang W, Yu W, Lin Y, Zhang T, Yao J, Zhou L, Zeng Y, Li H *et al* (2010) Regulation of cellular metabolism by protein lysine acetylation. *Science* 327: 1000–1004
7. Lin H, Su X, He B (2012) Protein lysine acylation and cysteine succination by intermediates of energy metabolism. *ACS Chem Biol* 7: 947–960
8. Peng C, Lu Z, Xie Z, Cheng Z, Chen Y, Tan M, Luo H, Zhang Y, He W, Yang K *et al* (2011) The first identification of lysine malonylation substrates and its regulatory enzyme. *Mol Cell Proteomics* 10: M111.012658
9. Xie Z, Dai J, Dai L, Tan M, Cheng Z, Wu Y, Boeke JD, Zhao Y (2012) Lysine succinylation and lysine malonylation in histones. *Mol Cell Proteomics* 11: 100–107
10. Tan M, Peng C, Anderson KA, Chhoy P, Xie Z, Dai L, Park J, Chen Y, Huang H, Zhang Y *et al* (2014) Lysine glutarylation is a protein post-translational modification regulated by SIRT5. *Cell Metab* 19: 605–617
11. Montellier E, Rousseaux S, Zhao Y, Khochbin S (2012) Histone crotonylation specifically marks the haploid male germ cell gene expression program: post-meiotic male-specific gene expression. *BioEssays* 34: 187–193
12. Tan M, Luo H, Lee S, Jin F, Yang JS, Montellier E, Buchou T, Cheng Z, Rousseaux S, Rajagopal N *et al* (2011) Identification of 67 histone marks and histone lysine crotonylation as a new type of histone modification. *Cell* 146: 1016–1028
13. Chen Y, Sprung R, Tang Y, Ball H, Sangras B, Kim SC, Falck JR, Peng J, Gu W, Zhao Y (2007) Lysine propionylation and butyrylation are novel

post-translational modifications in histones. *Mol Cell Proteomics* 6: 812 – 819

14. Guan KL, Xiong Y (2011) Regulation of intermediary metabolism by protein acetylation. *Trends Biochem Sci* 36: 108 – 116
15. Hirschey MD, Shimazu T, Huang JY, Schwer B, Verdin E (2011) SIRT3 regulates mitochondrial protein acetylation and intermediary metabolism. *Cold Spring Harb Symp Quant Biol* 76: 267 – 277
16. Lundby A, Lage K, Weinert BT, Bekker-Jensen DB, Secher A, Skovgaard T, Kelstrup CD, Dmytriyev A, Choudhary C, Lundby C *et al* (2012) Proteomic analysis of lysine acetylation sites in rat tissues reveals organ specificity and subcellular patterns. *Cell Rep* 2: 419 – 431
17. Park J, Chen Y, Tishkoff DX, Peng C, Tan M, Dai L, Xie Z, Zhang Y, Zwaans BM, Skinner ME *et al* (2013) SIRT5-mediated lysine desuccinylation impacts diverse metabolic pathways. *Mol Cell* 50: 919 – 930
18. Rardin MJ, He W, Nishida Y, Newman JC, Carrico C, Danielson SR, Guo A, Gut P, Sahu AK, Li B *et al* (2013) SIRT5 regulates the mitochondrial lysine succinylome and metabolic networks. *Cell Metab* 18: 920 – 933
19. Nishida Y, Rardin MJ, Carrico C, He W, Sahu AK, Gut P, Najjar R, Fitch M, Hellerstein M, Gibson BW *et al* (2015) SIRT5 regulates both cytosolic and mitochondrial protein malonylation with glycolysis as a major target. *Mol Cell* 59: 321 – 332
20. Weinert BT, Scholz C, Wagner SA, Iesmantavicius V, Su D, Daniel JA, Choudhary C (2013) Lysine succinylation is a frequently occurring modification in prokaryotes and eukaryotes and extensively overlaps with acetylation. *Cell Rep* 4: 842 – 851
21. Du J, Zhou Y, Su X, Yu JJ, Khan S, Jiang H, Kim J, Woo J, Kim JH, Choi BH *et al* (2011) Sirt5 is a NAD-dependent protein lysine demalonylase and desuccinylase. *Science* 334: 806 – 809
22. Yu J, Sadhukhan S, Noriega LG, Moullan N, He B, Weiss RS, Lin H, Schoonjans K, Auwerx J (2013) Metabolic characterization of a Sirt5 deficient mouse model. *Sci Rep* 3: 2806
23. Liu L, Peritore C, Ginsberg J, Shih J, Arun S, Donmez G (2015) Protective role of SIRT5 against motor deficit and dopaminergic degeneration in MPTP-induced mice model of Parkinson's disease. *Behav Brain Res* 281: 215 – 221
24. Nicklas WJ, Youngster SK, Kindt MV, Heikkila RE (1987) MPTP, MPP^+ and mitochondrial function. *Life Sci* 40: 721 – 729
25. Williams AC, Ramsden DB (2005) Autotoxicity, methylation and a road to the prevention of Parkinson's disease. *J Clin Neurosci* 12: 6 – 11
26. Langston JW, Ballard P, Tetrud JW, Irwin I (1983) Chronic Parkinsonism in humans due to a product of meperidine-analog synthesis. *Science* 219: 979 – 980
27. Boylston JA, Sun J, Chen Y, Gucek M, Sack MN, Murphy E (2015) Characterization of the cardiac succinylome and its role in ischemia-reperfusion injury. *J Mol Cell Cardiol* 88: 73 – 81
28. Slater EC (1967) An evaluation of the Mitchell hypothesis of chemiosmotic coupling in oxidative and photosynthetic phosphorylation. *Eur J Biochem* 1: 317 – 326
29. Maro B, Bornens M (1982) Reorganization of HeLa cell cytoskeleton induced by an uncoupler of oxidative phosphorylation. *Nature* 295: 334 – 336
30. Maro B, Marty MC, Bornens M (1982) *In vivo* and *in vitro* effects of the mitochondrial uncoupler FCCP on microtubules. *EMBO J* 1: 1347 – 1352
31. Page MM, Robb EL, Salway KD, Stuart JA (2010) Mitochondrial redox metabolism: aging, longevity and dietary effects. *Mech Ageing Dev* 131: 242 – 252
32. Wagner GR, Payne RM (2013) Widespread and enzyme-independent Nepsilon-acetylation and Nepsilon-succinylation of proteins in the chemical conditions of the mitochondrial matrix. *J Biol Chem* 288: 29036 – 29045
33. Ceccarelli C, Grodsky NB, Ariyaratne N, Colman RF, Bahnson BJ (2002) Crystal structure of porcine mitochondrial $NADP^+$-dependent isocitrate dehydrogenase complexed with $Mn2^+$ and isocitrate. Insights into the enzyme mechanism. *J Biol Chem* 277: 43454 – 43462
34. Harman D (1956) Aging: a theory based on free radical and radiation chemistry. *J Gerontol* 11: 298 – 300
35. Larsen PL (1993) Aging and resistance to oxidative damage in *Caenorhabditis elegans*. *Proc Natl Acad Sci USA* 90: 8905 – 8909
36. Vanfleteren JR (1993) Oxidative stress and ageing in *Caenorhabditis elegans*. *Biochem J* 292(Pt 2): 605 – 608
37. Schriner SE, Linford NJ, Martin GM, Treuting P, Ogburn CE, Emond M, Coskun PE, Ladiges W, Wolf N, Van Remmen H *et al* (2005) Extension of murine life span by overexpression of catalase targeted to mitochondria. *Science* 308: 1909 – 1911
38. Rebrin I, Forster MJ, Sohal RS (2007) Effects of age and caloric intake on glutathione redox state in different brain regions of C57BL/6 and DBA/2 mice. *Brain Res* 1127: 10 – 18
39. Rush GF, Gorski JR, Ripple MG, Sowinski J, Bugelski P, Hewitt WR (1985) Organic hydroperoxide-induced lipid peroxidation and cell death in isolated hepatocytes. *Toxicol Appl Pharmacol* 78: 473 – 483
40. Glorioso C, Oh S, Douillard GG, Sibille E (2011) Brain molecular aging, promotion of neurological disease and modulation by sirtuin 5 longevity gene polymorphism. *Neurobiol Dis* 41: 279 – 290
41. Zerez CR, Moul DE, Gomez EG, Lopez VM, Andreoli AJ (1987) Negative modulation of Escherichia coli NAD kinase by NADPH and NADH. *J Bacteriol* 169: 184 – 188
42. Wagner TC, Scott MD (1994) Single extraction method for the spectrophotometric quantification of oxidized and reduced pyridine nucleotides in erythrocytes. *Anal Biochem* 222: 417 – 426

